Semiconductor Optoelectronics, *Vol. 42 No. 2 (2023), 1030-1041*
https://bdtgd.cn/

Semiconductor Optoelectronics
ISSN: 1001-5868

“SNO_2-ZNO NANOCOMPOSITE SYNTHESIS AND CHARACTERIZATION PRODUCED CONFIDENT CONDUCTING POLYMERS FOR SENSING APPLICATIONS”

Ms. Ebhad Swagat Sadashiv
Dr. APJ Abdul Kalam University,Indore,MP, India, Department of Physics
swagatebhad1@gmail.com

Dr. Mohan N Giriya
Dr. APJ Abdul Kalam University,Indore,MP, India.
mohangiriya@gmail.com

Abstract: This reduced light transmission and increased energy loss.
Synthesis, self-assembly, and ZnO nanostructure and nanocomposites properties were examined. Chapters include zinc oxide nanoparticle production, characterization, and use. Order of this chapter: In the first half, asymmetric ZnO nanostructures with an interior cavity are examined. Structurally anisotropic nanostructures have newly formed inner spaces in their top areas. Different from nanostructures' hollow interiors. Surfactants may control fundamental nano-crystallites and two or more crystal planes in ZnO asymmetric nanostructures. As advised.

Hydrothermal processing created hourglass-shaped ZnO nanostructures. Scientists discovered ZnO subunits' structure and self-assembly method using Tween-85. Hour-glass structures are linearly assembled by van der Waals interactions between subunits' surface-anchored alkylated oleate groups. Van der Waals interaction on surfaces enabled this finding. This came to light after hourglass buildings were disassembled.
Keywords: *Substance Characteristics, ZnO Oxide, Synthesis, Nanostructure, and Nanocomposites*

INTRODUCTION

We synthesized ZnO and SnO_2 nano-composites by sol gel synthesis and examined their structural, morphological, and electrochemical properties. X-rays measure composite composition-based particle size and strain. As SnO_2 content increases, AFM shows a mainly homogeneous and granular surface.

Optical experiments using photoluminescence. Doped samples peak-shifted somewhat more than un-doped ones. Doping the host matrix and altering nano-composites' band gap energies triggered the shifting.
SnO_2–ZnO nanocomposite is synthesized at room temperature using SILAR. XRD patterns of

annealed films show SnO_2-ZnO nanocomposite formation. SEM displays SnO_2–ZnO nanocomposite's porous nanoparticle network. ZnO is cauliflower-shaped, SnO_2 nanoparticle-like. Composite film elements are EDS-validated. LPG, ethanol, hydrogen sulfide, and ammonia were detected by SnO_2–ZnO nano-composite sensors.

When SnO_2 ratio was increased, light communication decreased and energy loss rose. This was because the ratio reduced energy loss.

This work focused on ZnO-related nanostructures and nanocomposites production, self-assembly, and properties. This doctoral thesis was compulsory reading and writing. The nine chapters of this thesis describe zinc oxide nanoparticle creation, characterization, and application methodically. The chapters are ordered as follows: Chapters are presented in this order: Asymmetric ZnO nanostructures with cavities are examined in the first half of this article. New structural anisotropy was found in the upper half of nanostructures with the newly created internal space. Nanotube-based nanostructures enabled this discovery.

Hydrothermal method made hourglass-shaped ZnO nanostructures. Assembly accomplished its goal. Researchers used Tween-85 to identify ZnO subunits' unique structure and self-assembly. Van der Waals contact of surface-anchored alkylated oleate groups causes hour-glass structures to assemble linearly. Hour-glass structures are linearly assembled via van der Waals contact. This was identified because van der Waals interactions are surface-anchored. This was discovered when the hourglass-shaped buildings collapsed.

Material Science and Engineering's ability to create new materials has transformed society. Thin film technology powers cutting-edge gadgets. Modern high-tech relies on thin film science and technology. Grove found that sputtering cathode with high-energy positive ions formed metal sheets. Thin device films have been made for 40 years. Many real-world problems require two-dimensional thin films.

Their surface functionalities are the same as bulk materials, yet they cost less. The nature, functionality, and new properties of thin films have been used to create new technologies. Thin film technology is growing daily as new technologies shrink to atoms and achieve tolerances only an electron microscope can read. Films are solids between two planes and extended in two dimensions, but limited in a third direction perpendicular to XY.

This creates modest localized warmth. When developing metal coating methods for thin plastic products, substrates often melt during first deposition cycles. Monitor source-to-substrate distances and deposition rates to coat temperature-sensitive substrates. Charge vaporization occurs via induction, electric resistance, and electron beam heating. Thin layers can be deposited using laser ablation, cathodic arc, and thermal methods Laser beams pass through a glass to focus on evaporated powder from outside the evaporation system.

Interfacial nano-control makes nanocomposites. Controlling molecular interface, structure, and morphology is the goal. Chemical/physical qualities and functions may be unattainable separately. Nanocomposite domain sizes, topologies, and assembly must be tuned.

Solution solidifies using sol–gel. Sol-gel uses inorganic (chlorides, nitrates, sulfides) and metal organic precursors (alkoxide, acetylacetonate). Alkoxide precursor technique is flexible. Both hydrolysis and condensation cross-link molecular precursors. Zinc oxide, titania, and indium oxide develop at moderate temperatures.

Summary

This thesis aims to create, study, and use nanomaterials.

The study devised a nanocomposite to fix it. Nano-ZnO/SnO_2 co-precipitate. DLS, XRD, FTIR, SEM. Surface area of nanocomposites increased decolorization at wastewater concentration, catalyst quantity, and time. Time varied, but all experiments removed dye. High nanocomposite and low methylene blue minimized decolorization.

Nanorods in a nanoparticle matrix improve gas adsorption sites, making this material suitable for room-temperature gas detection with fast reaction and recovery.

RGO boosts photoexcited electron transport and material surface area, PANI increases light and dye absorption, and ZnO synergistically improves this. More efficient photocatalysts clean the environment.

Aluminum-doped ZnO nanoparticles were studied. In-situ polymerization produced Al-doped PPY-ZnO nanocomposites. Composites characterized by DSC, FT-IR, XRD, TGA. All composite samples expand and peak shift to lower wave numbers, indicating better conjugation and chemical interaction. Al-doped zinc oxide nanoparticles enhance composite conductivity, compactness, and conformation. Composites of amorphous polypyrrole with Al-doped ZnO nanoparticles.

Structure, thermal stability, surface morphology, optical, and electrical properties were examined. Studying optics, morphology, structure. The hexagonal wurtzite particles are 124.73, 48.51, and 80.69 nm. Agglomerate/granulate SEM images. FT-IR shows ZnO metal–oxygen, aluminum–oxygen, and metal–oxygen–aluminum bands.

This study hydrothermally generated p–n heterojunction SnO_2–SnO nanostructures in one pot. We used X-rays and electron microscopes on nanocomposite. n-SnO_2 nanocrystals on p-SnO crystals formed p–n heterojunctions. SnO_2–SnO composite gas sensors detected NO_2 better at 50 °C. p–n heterojunctions detect NO_2. Low-temperature NO_2 sensor SnO_2–SnO p–n. In situ-grown SnO_2 nanocrystals on SnO nanoplates improved sensor response. This research makes NO_2 and gas detectors.

Although pure SnO_2 nanoparticles possessed small grain sizes and large surface areas, they were poor NO_2 sensors. SnO_2–SnO heterojunctions may lower temperature and improve sensing. P–n heterojunction semiconductors detect gases well.

CBD used zinc sulfate ($ZnSO_4$), ethylenediamine (C_2H8N_2), and sodium hydroxide to make ZnO thin films on glass slides. The films were structurally, morphologically, and optically evaluated. SEM nanorod assemblies.

The suggested growth method can create aligned ZnO nanorod arrays at scale without expensive or accurate vacuum equipment.

The work uses photochemistry to make Ag/SnO_2 composites. UV-induced silver nitrate photoreduction produces in situ Ag nanoparticles.

Researching compound $AgNO_3$ solutions. Under metal halide lamps, composites photodegraded aqueous methyl orange. Photocatalytic Ag/SnO_2 composites have enough silver.

Researching photocatalysis, composition, and morphology. Photoelectrons separate electrons and holes in SnO_2 silver. Ag nanoparticles boost SnO_2 photocatalysis. 3mM $AgNO_3$ Ag/SnO_2 composites degrade MO best. The synthesis of noble nanoparticle-loaded semiconductor photocatalysts is photochemical.

Table: Comparison of the photodegradation efficiency of methylene blue on pure ZnO and modified ZnO NPs

Material	**Dye**	**Light**	***E* (%)**
ZnO Sn^{4+}-doped ZnO (2%) ZnO ZnO–SnO_2(4%)	Methyl orange Ethyl 4-hydroxybenzoate bisphenol A Ethyl 4-hydroxybenzoate bisphenol A	VisibleUV	86 51 82
ZnO–SnO_2(4%) SnO_2 $ZnFe_2O_4$/SnO_2(10%) ZnO–SnO_2 ZnO	 methylene blue Methyl orange Methylene blue AR-183 dye	 Visible UV	95 39 44.83 38
ZnO–SnO_2 ZnO–SnO_2 rhodamine B	UV Visible	UV Visible	94 101.35 97.20

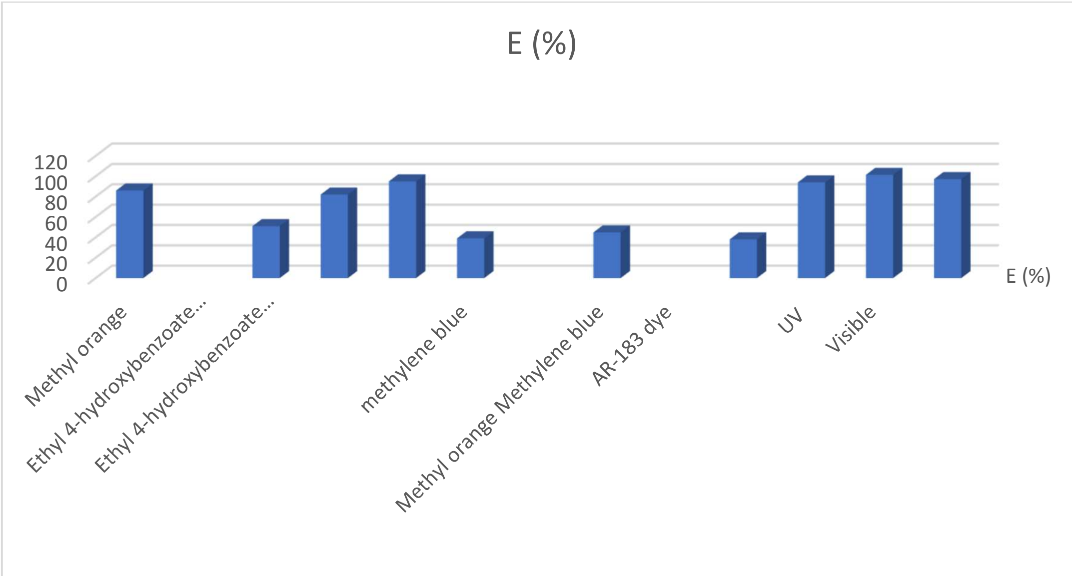

Graph: Comparison of the photodegradation efficiency of methylene blue on pure ZnO and modified ZnO NPs

Polymers for Sensing

Natural Rubber

India rubber, latex, Amazonian rubber, caucho, and caoutchouc are polymers of isoprene with trace amounts of other organic compounds as impurities. Latex, caucho, caoutchouc, and India rubber are other names for rubber. Elastomers include natural rubber polyisoprene.

Cellulose

Cellulose is a linear polysaccharide with the chemical formula n and several hundred to many thousands of -linked D-glucose units. Cellulose is organic.

Green plants, algae, and oomycetes have cellulose in their cell walls, which is structurally important.

Cellulose dissolves in several media, including commercial tech. Cellulose is regenerated from pulp using reversible dissolution.

Chlorinated Vinyl

Vinyl chloride is an organochloride identified by the formula $H_2C=CHCl$. Also called vinyl chloride, chloroethene, or monomer. Use this colorless industrial chemical to make poly. Vinyl chloride monomer is a top-20 petrochemical producer.

Organic vinyl chloride $H_2C=CHCl$. Known as VCM or chloroethene. Poly (vinyl chloride) manufacturing requires this colorless industrial chemical. A top-20 global petrochemical producer is vinyl chloride monomer. The US produces the most vinyl chloride due to inexpensive chlorine and ethylene. Vinyl chloride is widely used and produced in China.

Vinyl chloride burns, cancers, and smells wonderful. It comes from soil microbes decomposing chlorinated solvents. Industry-generated vinyl chloride and chlorinated chemical degradation harm air and water. Landfills contain vinyl chloride.

Polyaniline (Pani) Polymer

The semi-flexible rod polymer family includes conducting polymer and organic semiconductor polyaniline (PANI). Electrical conductivity and mechanical characteristics make the chemical interesting. One of the most researched conducting polymers is polyaniline.

A multi-stage emeraldine base model is suggested. The reaction starts with pernigraniline PS salt oxidation. Second, aniline monomer oxidizes to radical cation, converting pernigraniline to emeraldine salt.

Polyaniline is made as long-chain polymer aggregates, surfactant-stabilized nanoparticle dispersions, or stabilizer-free nanofiber dispersions, depending on supplier and synthetic method. Surfactant-stabilized polyaniline dispersions

Table: Average crystallite size of ZnO obtained from XRD

Sr. No.	Calcination Temperature (0C)	Crystallite size, D (nm)
1	350	76
2	550	84
3	750	142
4	950	191

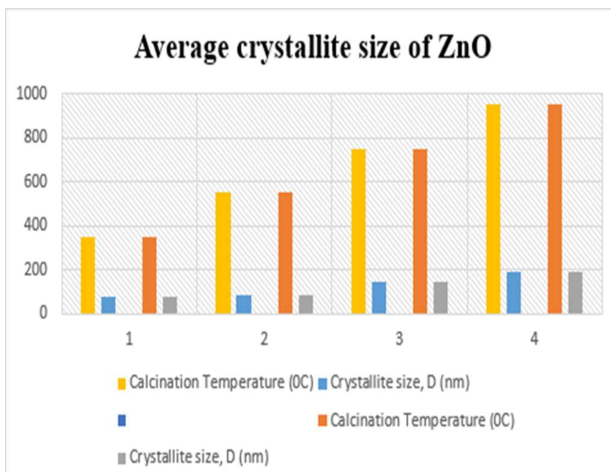

Graph: Average crystallite size of ZnO obtained from XRD

As the calcination temperature rises, the average crystallite size increases. When calcined at 950°C, there is a noticeable rise in crystallite size. Grain boundaries migrate at such high temperatures, resulting in the development of giant grains and the coalescence of small grains.

Table: Optical band gap of different ZnO samples calcined at different temperatures

Sr. No.	Calcination Temperature (C)	Band gap (eV)
1	350	3.34
2	560	3.28

3	780	3.27

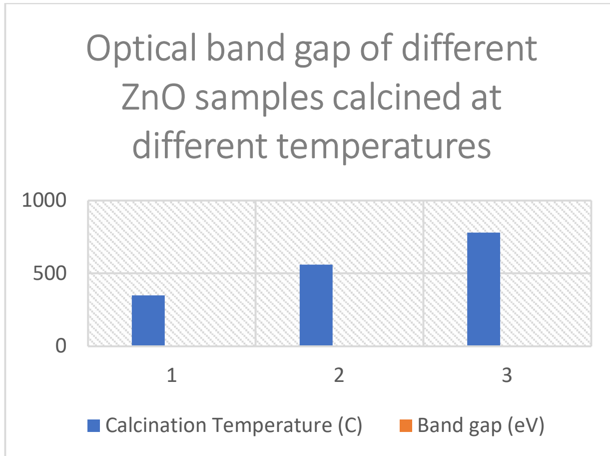

Graph: Optical band gap of different ZnO samples calcined at different temperatures

As the calcination temperature rises, the average crystallite size increases. When calcined at 950°C, there is a noticeable rise in crystallite size. Grain boundaries migrate at such high temperatures, resulting in the development of giant grains and the coalescence of small grains.

Table: Concentration of various elements in ZnO nanoparticles

Element	**Concentration**	**Statistical Error (%)**
Ti	1000 ppm	12.5
Fe	980 ppm	16.8
Zn	99.87%	0.19

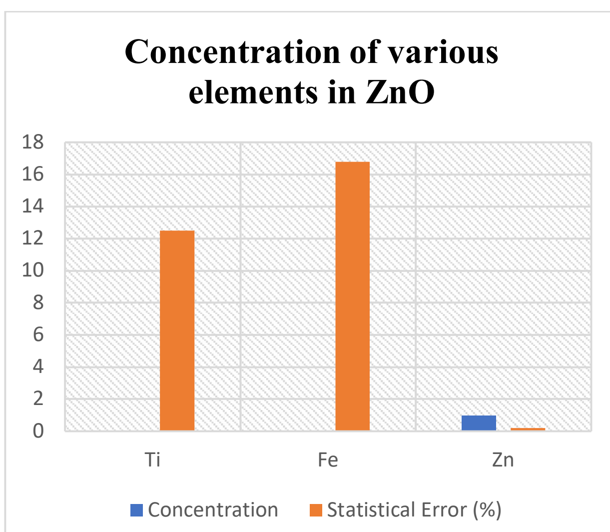

Graph: Concentration of various elements in ZnO nanoparticles

ZnO nanoparticles were made via a straightforward precipitation technique. The XRD and EDS measurements unequivocally show that the aforementioned procedure produces extremely pure ZnO. ZnO's SEM pictures demonstrate how the calcination temperature altered the material's shape. The produced material's excellent purity and the trace amounts of elements like Fe and Ti were validated by PIXE analysis. An increase in calcination temperature resulted in a decrease in ZnO's band gap and a shift in the absorption maxima toward higher wavelengths.

Table: Characteristics of SnO2–ZnO films obtained by solid-phase low-temperature

Materials	5SnO2–95ZnO	50SnO2–50ZnO	95SnO2–5ZnO
Ea, eV	0.98	1.29	1.97
Eg1, eV	4.34	3.58	4.05
Eg2, eV	3.79	3.01	3.98
D (XRD), nm	18	18	18
D (SEM), nm	14	12	19

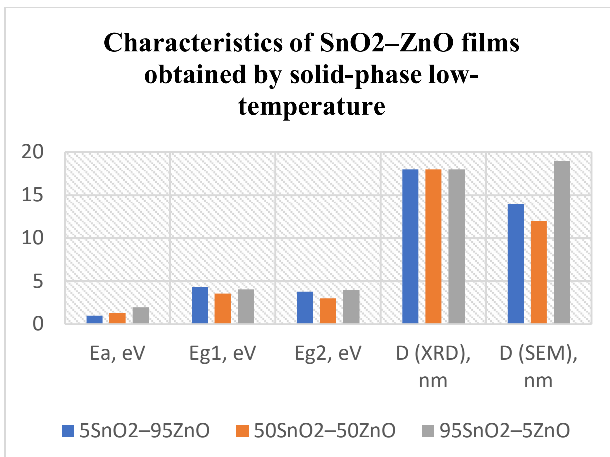

Graph: Characteristics of SnO2–ZnO films obtained by solid-phase low-temperature

Table: Crystallite size distribution of Eu doped ZnO/SnO_2 nanocomposite for different molar ratios of ZnO and SnO_2 and their lattice parameters

SnO_2	Scherrer	Williamson	$\varepsilon/10^{-4}$	*a=b*	*ca=b*	*c*
10:1	15–30	9.71	12.64	3.1750	5.1610 4.6122	3.0710
5:1	10–20	9.47	12.04	3.1503	5.1398 4.5628	3.0834
2:1	10–20	8.59	14.77	3.1945	5.1804 4.6481	3.1191
1:1	10–20	10.96	8.53	3.1843	5.1885 4.6208	3.1245
1:2	10–25	13.03	6.06	3.1713	5.1528	3.1236

					4.6058	
1:5	10–25	10.84	10.89	3.1762	5.2230 4.6199	3.2499
1:10	10–25	9.04	14.09	3.1393	5.1375 4.5756	3.1056

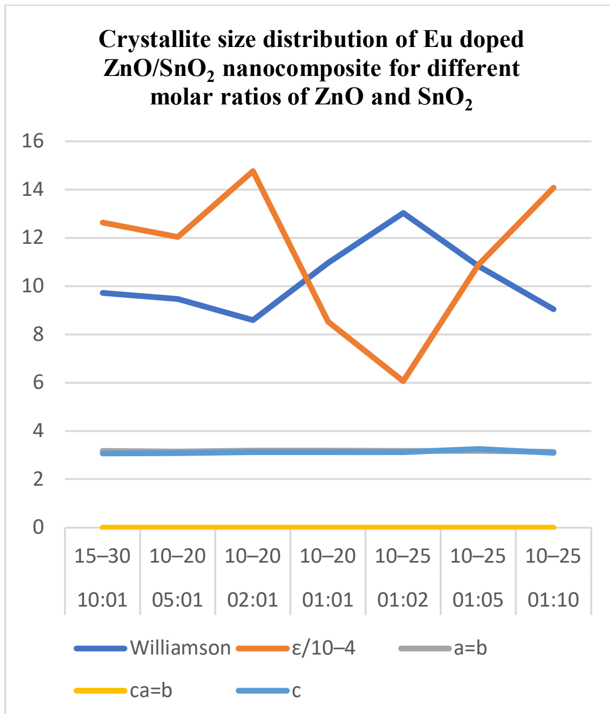

Graph: Crystallite size distribution of Eu doped ZnO/SnO_2 nanocomposite for different molar ratios of ZnO and SnO_2 and their lattice parameters

CONCLUSION

At 450°C for SnO2 and 300°C for ZnO, thin films are sprayed. SnO2 bottom layer thickness in bilayer ZnO/SnO2 thin films is measured. This research finds.

ZnO sprayed particles uniformly cover substrates, and the scanned region has fibrous and non-fibrous ZnO thin films. FESEM shows homogenous SnO2 film on glass. FESEM shows sprayed particles on glass. FESEM photos show agglomerated ZnO/SnO2 grains. SnO2's fibrous surface decreases with thickness. SnO2 and ZnO have distinct lattice fringes at the atomic contact.

ZnO, SnO2, and ZnO/SnO2 AFM images show tiny grains. 3D film growth fluctuated. SnO2 adds thickness. All developed films are NIR transparent, per UV-visible spectroscopy. 3.68 eV straight band gap in thin SnO2; larger bottom layer increases bilayer band gap. Bilayer thin film refractive index decreases with thickness.

Temperature decreases film resistance, indicating semi conductivity. Bilayer resistance decreases with thicker SnO2. Concentration or movement may induce this. Thicker SnO2 decreases bilayer thin film sheet resistance. Zn increases SnO2 carrier concentration.

Bilayer ZnO/SnO2 nano-composite thin films equal prior results in surface, structural, optical, and electrical properties. Bilayered films improved electrical and optical properties. ZnO/SnO2 bi-layer is in TCOs 129's solar and optoelectronic band gap. Single-layer ZnO/SnO2 film resistance was lower. AFM images showed a thick bilayer surface. Gas sensing and opto-electronics benefit from bi-layered ZnO/SnO2 film.

REFERENCES

1. Photo-Catalytic degradation of Methylene blue by ZnO/SnO_2 nanocomposite Samad Sabbaghi, Fateme Doraghi, J. Water Environ. Nanotechnology, 2016
2. Biological synthesis of nano composite SnO2 – ZnO – Screening for efficient photocatalytic degradation and antimicrobial activity, S. Sudhaparimala, M. Vaishnavi, ScienceDirect, Materials Today: Proceedings, ELSEVIER, 2016
3. UV-assisted synthesis of reduced graphene oxide zinc sulfide composite with enhanced photocatalytic activity, Koushik Chakraborty, Sankalpita Chakrabarty, Poulomi Dasb, Surajit Ghosh, Tanusri Pal, Materials Science and Engineering B, ELSEVIER, 2016
4. Investigation on Structural, Surface Morphological and Dielectric Properties of Zn-doped SnO_2 Nanoparticles Suresh Sagadevana and Jiban Podderb, Materials Research 2016
5. Construction of 1D SnO2-coated ZnO nanowire heterojunction for their improved n-butylamine sensing performances, Liwei Wang, Jintao Li, Yinghui Wang, Kefu Yu, Xingying Tang, Yuanyuan Zhang, Shaopeng Wang & Chaoshuai Wei, Scientific Reports 2016
6. ZnO/SnO2/Zn2SnO4 nanocomposite: preparation and characterization for gas sensing applications, M. Chitra1, K. Uthayarani, N. Rajasekaran, N. Neelakandeswari2, E. K. Girija, D. Pathinettam Padiyan, Nanosystems: Physics, Chemistry, Mathematics, 2016
7. Study On The Activity of ZnO-SnO2 Nanocomposite Against Bacteria And Fungi Title: Karzanabdulkareem Omar, Bashdar Ismael Meena, Srwa Ali Muhammed, Physicochem. Probl Miner. Process, 2016
8. A new ZnO/rGO/polyaniline ternary nanocomposite as photo catalyst with improved photocatalytic activity, Author: Huipeng Wu Shengling Lin Chuanxiang Chen Wei Liang Xiaoyan Liu Hongxun Yang, Accepted Manuscript, 2016
9. Synthesis and Studies on Nanocomposites of polypyrrole-Al-doped zinc oxide Nanoparticles V.T. Bhugul, G.N. Choudhari, International Journal of Scientific and Research Publications, 2015
10. Fabrication of SnO2–SnO nanocomposites with p–n heterojunctions for the low-temperature sensing of NO2 gas, Lei Li, Chunmei Zhang and Wei Chen, Nanoscale, 2015
11. Growth of ZnO Nanorods on Glass Substrate by Chemical Bath Deposition, S. Rezabeigy, M. Behboudniaa, N. Nobari, 5th International Biennial Conference on Ultrafine Grained and Nanostructured Materials, UFGNSM15, ScienceDirect, Elsevier, 2015
12. Photochemical Preparation of Ag/SnO Composites and their Photocatalytic Properties, Hongjuan Wang, Wenlong Li, International Conference on Chemical, Material and Food Engineering (CMFE-2015)
13. Structural and spectroscopic diagnosis of ZnO/SnO2 nanocomposite influenced by Eu3+ Pankaj Kr. Baitha, J. Manam, Elsevier, Journal of Rare Earths, 2015

14. Sol–gel synthesis of ZnO–SnO2 nanocomposites and their morphological, structural and optical properties, Suresh Kumar Ravi Nigam Virender Kundu Neena Jaggi, J Mater Sci: Mater Electron, 2015
15. Development, optimization and characterization of a twostep sol–gel synthesis route for ZnO/SnO2 nanocomposite, Isha Das, Suresh Sagadevan, Zaira Zaman Chowdhury, Md. Enamul Hoque, Journal of Materials Science: Materials in Electronics 2017
16. Synthesis of SnO2 and ZnO Nanoparticles and SnO2-ZnO Hybrid for the Photocatalytic Oxidation of Methyl Orange, A. Ghaderi, S. Abbasi, F. Farahbod, 2015
17. Growth of ZnO Nanorods on Glass Substrate by Chemical Bath Deposition, S. Rezabeigy, M. Behboudnia, N. Nobari, 5th International Biennial Conference on Ultrafine Grained and Nanostructured Materials, ScienceDirect, Elsevier, Procedia Materials Science, 2015
18. Gas sensing properties of zinc stannate (Zn2SnO4) nanowires prepared by carbon assisted thermal evaporation process, T. Tharsika, A.S.M.A. Haseeb, S.A. Akbar, M.F.M. Sabri, Y.H. Wong, Journal of Alloys and Compounds, Elsevier, 2015
19. Synthesis, Characterization and Photocatalytic Activity of Mg-Impregnated ZnO–SnO2 Coupled Nanoparticles, Mohammad A. Behnajady and Yasamin Tohidi, Photochemistry and Photobiology, 2014
20. Structural and optical properties of SnO2 nano towers and interconnected nanowires prepared by carbothermal reduction method, Neha Bhardwaj, Sini Kuriakose, S. Mohapatra, Journal of Alloys and Compounds, Elsevier, 2014
21. Structural and optical properties of ZnO–SnO2 mixed thin films deposited by spray pyrolysis, T. Tharsika, A.S.M.A. Haseeb, M.F.M. Sabri, Thin Solid Films, ELSEVIER, 2014
22. Hierarchical electrospun nanofibers for energy harvesting, production and environmental remediation, Palaniswamy Suresh Kumar, Jayaraman Sundaramurthy, Subramanian Sundarrajan, Veluru Jagadeesh Babu, Gurdev Singh, Suleyman I. Allakhverdiev and Seeram Ramakrishna, Energy Environ. Sci., 2014
23. Effects of MeV ion irradiation on structural and optical properties of SnO2–ZnO nanocomposites prepared by carbothermal evaporation, Neha Bhardwaj, Sini Kuriakose, A. Pandey, R.C. Sharma, D.K. Avasthi, Satyabrata Mohapatra, Journal of Alloys and Compounds, Elsevier, 2014
24. Improvement sensitivity humidity sensor based on ZnO/SnO2 cubic structure, N.D. Md Sin, S. Ahmad1, M.F. Malek, M.H. Mamat, M. Rusop, IOP Conf.Series: Materials Science and Engineering, 2013
25. Synthesis and characterization of SnO2 Nanoparticles for PV Applications, Saira Riaz, Adeela Nairan and Shahzad Naseem, 2013
26. Synthesis, Characterization, and Activity of Tin Oxide Nanoparticles: Influence of Solvothermal Time on Photocatalytic Degradation of Rhodamine B, Zuoli He, Jiaqi Zhou, Modern Research in Catalysis, 2013
27. Optically stimulated piezooptical effects in Cu-doped ZnO filmsE.M El Jald, V.A. Franiv, A. Belayachi, M. Abd-Lefdil, Optik, elsevier, 2013
28. Influence of K-doping on the optical properties of ZnO thin films grown by chemical bath deposition method G. Shanmuganathan, I.B. Shameem Banu, S. Krishnan, B. Ranganathan, Journal of Alloys and Compounds, elsevier, 2013

29. Low temperature sensing of NO2 gas using SnO2-ZnO nanocomposite sensor, Rakesh Kumar Sonker, Anjali Sharma, Md. Shahabuddin, Monika Tomar, Vinay Gupta, Advanced Materials Letters, 2013
30. Preparation of Cauliflower-like ZnO Films by Chemical Bath Deposition: Photovoltaic Performance and Equivalent Circuit of Dye-sensitized Solar Cells, Yuqiao Wang, Xia Cui, Yuan Zhang, Xiaorui Ga, Yueming Sun, SciVerse ScienceDirect, J. Mater. Sci. Technol, Elsevier, 2013
31. Preparation, Characterization, and Photocatalytic Activity of TiO2/ZnO Nanocomposites, LiqinWang, Xiujun Fu, Yang Han, E. Chang, HaitaoWu, Haiying Wang, Kuiying Li, and Xiaowen Qi, Hindawi Publishing Corporation Journal of Nanomaterials, 2013
32. Characterization of Chemically Synthesized Polyaniline-Zinc Oxide Nanocomposites, Ganesh R. Yerawar, Der Pharma Chemica, 2012,
33. Synthesis and Characterization of CeO-ZnO Nanocomposites Ashwani Sharma, Pallavi, Sanjay Kumar, Nanoscience and Nanotechnology 2012
34. Preparation of cobalt oxide/zinc oxide nanocomposite, L. Nikzad, M. R. Vaezi and S. Alibeigi, A.Esmaielzadeh Kandjani, 2010
35. Nanocomposite ZnO–SnO2 Nanofibers Synthesized by Electrospinning Method Kandasami Asokan • Jae Young Park, Sun-Woo Choi, Sang Sub Kim, Nanoscale Res Lett (2010)
36. Nanocomposites: Synthesis, Structure, Properties and New Application Opportunities, Pedro Henrique Cury Camargo, Kestur Gundappa Satyanarayana, Fernando Wypych, Materials Research, 2009
37. Effects of Sol concentration on the structural and optical properties of SnO2 Nanoparticle, Ali Reza Razeghizadeh Iraj Kazeminezhad, Lila Zalaghi, Vahdat Rafee
38. Graphene/TiO2 Nanocomposites: Synthesis Routes, Characterization, and Solar Cell Applications Chin Wei Lai, Foo Wah Low, Siti Zubaidah Binti Mohamed Siddick and Joon Ching Juan,
39. Synthesis and Characterization of CoO-ZnO-Based Nanocomposites for Gas-Sensing Applications, Parthasarathy Panchatcharam,
40. Molten-Salt Flux Mediated Synthesis of ZnO-SnO2 composites: Effects of Surface Areas and Crystallinities on Photocatalytic Activity, Rachelle Austin, Feier Hou,
41. Solid-state synthesis and optical properties of ZnO and SnO2 nanoparticles and their nanocomposites with SiO2, C. Diaz, M. L.Valenzuela, M. Segovia, K. Correa, R. de la Campa and A. Presa Soto,